

Investigation into the nanostructural evolution of TiO₂-polymethyl methacrylate nanohybrids derived from the sol-gel technique

Akhmad Herman Yuwono^{1*}, Donantha Dhaneswara¹
Yu Zhang² and John Wang²

¹Department of Metallurgy and Materials Engineering, Faculty of Engineering
University of Indonesia, Depok-West Java, Indonesia 16424
Tel : +(62-21) 7863510. Fax : +(62-21) 7872350
E-mail : ahyuwono@@metal.ui.ac.id

²Department of Materials Science and Engineering Faculty of Engineering
National University of Singapore, Singapore 117574
E-mail : msewangj@nus.edu

ABSTRACT

In this research, the nanostructural evolution of TiO₂ crystallite upon in situ sol-gel process of titania-polymethyl methacrylate (TiO₂-PMMA) nanocomposites was systematically investigated. The main objective is to understand the mechanisms responsible for the amorphous nature of the sol-gel derived TiO₂-polymethyl methacrylate (PMMA) nanohybrids. For this purpose, two sol-gel parameters i.e. the coupling agent concentration, water content or hydrolysis ratio (rw), and pH value of the titania precursor solution were varied. On the basis of XRD analysis, it has been found that the modification of those parameters can enhance the nanocrystallinity of pure TiO₂ phase. However, this could not be applied when the titania precursor was mixed with the PMMA segment. On the basis of XRD and FTIR analyses, it was found that the largely amorphous TiO₂ state is related to the fast development of stiff Ti-OH networks during the hydrolysis and condensation stages in sol-gel process, worsened by the entrapment of the rigid PMMA matrix.

Keywords

Example:
Nanohybrids, TiO₂, PMMA, hydrolysis ratio, pH, nanostructural evolution.

1. INTRODUCTION

Poly(methylmethacrylate) or PMMA is well-known as an excellent optical polymer for use in optical fibers, optical disks and lenses [1]. However, the refractive index (n_o) of PMMA is limited to only 1.49. On the other hand, titanium oxide (TiO₂, titania) has been recognized as an inorganic material having high refractive index, i.e. ~2.45 (anatase) and ~2.70 (rutile). Therefore, an incorporation of TiO₂ nanoparticles into PMMA has been considered for preparing high-refractive index polymers. Accordingly, titania-poly(methyl methacrylate) or TiO₂-PMMA nanohybrids have been studied previously by several researchers. Zhang *et al.* [2] synthesized TiO₂-PMMA nanohybrid using chelating ligand as a coupling agent. A further study on preparation and optical properties of PMMA-titania thin films was performed by Chen *et al.*, [3,4] who synthesized thin film TiO₂-PMMA nanocomposites by *in situ* sol-gel process of trialkoxysilane-capped PMMA-titania combined with spin coating and multi-step annealing process. The refractive indices of thus prepared films were reported in the range of 1.505-1.867, provided the loading of titanium alkoxide in the precursor solution was up to 90 wt%.

In our previous works, it has been shown that the TiO₂-PMMA nanohybrids derived from *in situ* sol-gel polymerization exhibits a very fast recovery time of ~1.5 picosecond and a large third order nonlinear optical susceptibility, $\chi^{(3)}$, as observed [5,6]. Therefore, the nanocomposites are promising for several potential applications in optoelectronic devices such as nonlinear optical switching devices in photonics and real-time

coherent optical signal processors [7,8]. However, it is realized, that TiO₂-PMMA nanohybrids are limited by the occurrence of amorphous TiO₂ nanoparticles, which cannot be avoided under the conditions tolerable by the polymer matrix upon the low temperature sol-gel process. Therefore, it is thus of our main interest to investigate the factors causing the amorphous nature of TiO₂ phase in PMMA matrix. For this purpose, two synthesis parameters involved in the *in situ* sol-gel polymerization, including the water content or hydrolysis ratio (*r_w*), and pH value of the titania precursor solution were systematically investigated.

2. EXPERIMENTAL

In this work, we used an *in-situ* sol-gel polymerization technique, which is basically a thorough mixing process between a pre-hydrolyzed TiO₂ precursor (titanium isopropoxide, Ti-iP) and pre-polymerized PMMA. First, the monomers, methyl methacrylate (MMA, 99%, Acros) and coupling agent 3-(trimethoxysilyl)propyl methacrylate (MSMA, 98%, Acros), and initiator benzoyl peroxide (BPO, 98%, Acros) in solvent tetrahydrofuran (THF, 99%, Acros) were added into a reaction flask and polymerized at 60°C for 1 hour. The molar ratio of MSMA to MMA+MSMA was controlled at 0.25 and the amount of BPO added to the mixture was fixed at 3.75 mol%. Furthermore, a TiO₂ based sol solution was prepared by mixing titanium isopropoxide (Ti-iP, 98%, Acros) with ethyl alcohol (EtOH, 95%, Merck) in a container and stirred for 30 minutes. A mixture of de-ionized water and hydrochloric acid (HCL, 36%, Ajax) was then added under stirring condition into the transparent solution to promote hydrolysis. The Ti-iP concentration in the solution was controlled at 0.4 M. It should be noted that for investigation purposes, first we varied the coupling agent concentration since this agent governs the interaction between inorganic and organic moieties in nanohybrids. For further investigation, three different sols with different pH value i.e. 3.08, 1.08 to 0.33 were prepared under the same ratio of water to Ti-iP (*r_w*) or hydrolysis ratio of 0.82. At the same time, other sols with varying hydrolysis ratio of 0.82, 2.00 and 3.50 under the same pH value of 0.78 were also synthesized. All of these parameters were thoroughly varied while maintaining the stability of sol solutions to be clear and transparent. Finally, this transparent sol

solution was carefully added drop by drop over a duration of 30 minutes into the partially polymerized monomers with rigorous stirring to avoid local inhomogeneities. The reaction was allowed to proceed at 60°C for another 2 hours. In this study, the weight ratio between the inorganic and organic precursors in the reaction mixture was fixed at 60:40.

The fabrication of thin film was performed by spin coating the hybrid solution onto glass substrates at 3000 rpm for 20 seconds. The coated films were then annealed in two stages of curing temperatures, *i.e.* at 60°C for 30 minutes and 150°C for 3 hours. The nanohybrids characterization was carried out with X-ray diffraction (XRD) measurements on Bruker AXS θ -2 θ diffractometer using Cu K- α radiation (1.5406 Å) operated at 40 kV, 40 mA and with a step-size of 0.02° and time/step of 20 seconds. The incidence angle between the beam and film plane was fixed at 1.5°. Further analysis was performed using Fourier Transform Infrared (FTIR) spectroscopy at room temperature in the range of 4000-400 cm⁻¹ using Bio-Rad model QS-300 spectrometer, which has a resolution of ± 8 cm⁻¹.

3. RESULTS AND DISCUSSION

Effect of coupling agent concentration. In the present study, 3-(trimethoxysilyl)propyl methacrylate (MSMA) is introduced as a coupling agent between the inorganic titanium alkoxide precursor and the organic MMA matrix. In our previous work [5,6] a constant MSMA/(MSMA+MMA) molar ratio of 0.25 was used in the nanohybrid preparation. Thermal gravimetric analysis (TGA) and FTIR studies confirmed that the thus derived nanohybrids demonstrated a strong interaction between the inorganic and organic moieties. For optical properties, this can be beneficial since the resulting nanohybrid is transparent in the visible region. On the other hand, however, such a strong bonding may have a reverse effect on the TiO₂ formation, *i.e.*, the strong hindrance experienced by the hydrolyzed titanium alkoxide (Ti-OH networks) in PMMA gave rise to largely amorphous TiO₂ phase. Therefore it is of further interest to investigate whether an incorporation of a lower concentration of coupling agent at the solution preparation stage can provide a higher flexibility for the hydrolyzed titanium alkoxide to undergo densification in the PMMA matrix during the subsequent annealing process. By having so, it is expected that Ti-O-Ti bonds will be able to

develop a long-range order, such that nanocrystalline TiO₂ particles can be formed. The amount of MSMA/(MSMA+MMA) molar ratio was reduced down to 0.05 and the resulted nanohybrid was compared to that derived from 0.25

Figure 1 is the XRD traces for both nanohybrids showing two broadened phase peaks at 2θ angles of 25.35 and 48.12° that can be assigned to (101) and (200) crystal planes of anatase phase. The nanohybrid derived from the coupling agent ratio of 0.05 shows slightly stronger diffraction peaks than those derived from the coupling agent ratio of 0.25.

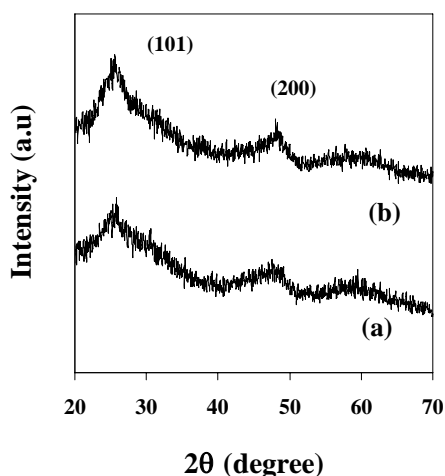


Figure 1. XRD traces of nanohybrid derived from ratio MSMA/(MSMA+MMA) ratio of (a) 0.25 and (b) 0.05.

For further confirmation, FTIR spectroscopy of the two nanohybrids was investigated. The stretching vibrations for both samples are shown in Figures 2 and 3, for both low wavenumber range (1100–400 cm⁻¹) and high wavenumber range (4000–2400 cm⁻¹), respectively. Figure 2 shows the occurrence of absorption bands located at 450 and 650 cm⁻¹ which can be assigned to Ti–O and Ti–O–Ti stretching vibrations, respectively as the characteristic of nanocrystalline TiO₂ in short and long range order [9,10]. In addition, there is an additional band at 910 cm⁻¹, corresponding to the stretching vibration of Ti–O–Si bond [11]. Although the two nanohybrids show similar intensities, however a careful comparison reveals that there occurs a considerably higher band intensity in the range of 1000–1200 cm⁻¹ in spectrum "(b)", in comparison to spectrum "(a)". This band, with the strongest absorption peak located at ~1080 cm⁻¹, is assigned

to the Ti–O–C stretching mode originated from the remaining unhydrolyzed alkoxy groups [12,13]. Although there is a possibility of overlapping with C–O–C bonds originated from the PMMA matrix in the range of 1039–1192 cm⁻¹ [3], however the same amount of MMA monomer was incorporated into both nanohybrids. This was further confirmed by checking the stretching vibration of C–H bond at 2950 cm⁻¹ as shown in Figure 3.15. Both spectra "(a)" and "(b)" are very similar in intensity. Therefore it can be concluded that the enhanced intensity at ~1080 cm⁻¹ in spectrum "(b)" of Figure 3.14 is related to the higher number of Ti–O–C bonds in the nanohybrid derived from the lower coupling agent ratio.

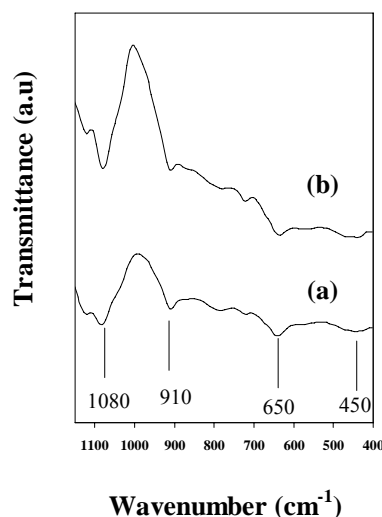


Figure 2. FTIR spectra of the nanohybrid derived from MSMA/ (MSMA+MMA) ratio of (a) 0.25 and (b) 0.05, respectively, in the low wavenumber range of 1100–400 cm⁻¹.

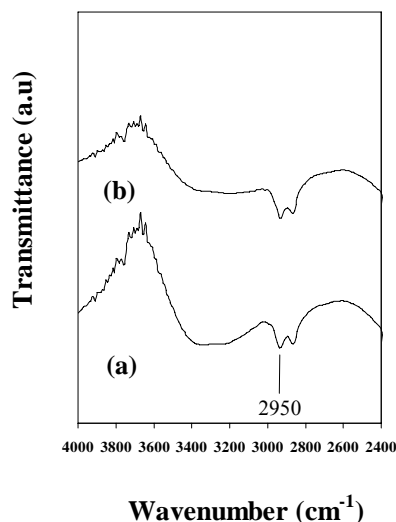


Figure 3. FTIR spectra of the nanohybrid derived from MSMA/(MSMA+MMA) ratio of (a) 0.25 and (b) 0.05, respectively, in the high wavenumber range of 4000–2400 cm^{-1} .

It is of further interest to investigate the reason behind the enhanced nanocrystallinity shown by the nanohybrid derived from the lower coupling agent ratio. One approach is to look at the three absorption bands, *i.e.* Ti–OH at $\sim 3400 \text{ cm}^{-1}$, Ti–O–C at 1080 cm^{-1} and Ti–O–Si at 910 cm^{-1} . As seen in Figure 3, the intensity of Ti–OH band for the nanohybrid derived from the coupling agent ratio of 0.05 is lower than that derived from 0.25, while a higher intensity of Ti–O–C band (Figure 2) is demonstrated by the former. In contrast to these differences, both nanohybrids show more or less the same intensity for Ti–O–Si band. As proposed by Brinker and Hurd [14] and Langlet *et al.* [15], the largely amorphous TiO_2 thin films obtained at low temperatures is due to the formation of stiff Ti–OH networks resulted from the fast condensation of titanium alkoxide precursor, which in turn hinder the densification of crystallite TiO_2 phase. In this connection, therefore, the low intensity of Ti–OH observed for the nanohybrid derived from the lower coupling agent ratio suggests a reduced amount of amorphous phase. On the other hand, the high intensity of Ti–O–C stretching mode from the unhydrolyzed alkoxy groups in this sample is related to the high number of interfacial sites for TiO_2 nucleation. The interfacial bond is not as stiff as Ti–OH network and is therefore sufficiently flexible to take part in the densification of TiO_2 phase, *i.e.*, by the arrangement of Ti–O–Ti bonds in the long-range order and thus an enhancement in TiO_2 nanocrystallinity was resulted, as detected by XRD. Zhang *et al.* [13] has reported that Ti–O–C bond, together with Ti–O and Ti–OH, can lead to connected networks of TiO_2 nanoparticles in titania-poly(phenylenevinylene) or TiO_2 -PPV nanocomposites. The interfacial phase plays an important role in providing the necessary dispersion function and thus preventing the agglomeration of TiO_2 nanoparticles in polyvinyl alcohol (PVA) matrix [16]. The effects of different coupling agent concentrations on nanohybrids were further investigated by TGA. Figure 4 shows that both samples have similar response upon heating up to 850 $^\circ\text{C}$. It is clearly demonstrated that the nanohybrid derived from the lower coupling agent ratio decomposes at a lower temperature than that

derived from the higher coupling agent ratio. This can be accounted for by the high number of interfacial Ti–O–C bonds of unhydrolyzed alkoxy groups in the former, as has been confirmed by FTIR spectroscopy. On the other hand, the similarity in TGA behavior up to 300 $^\circ\text{C}$ shown by both samples can be related to the similar intensity of Ti–O–Si band at 910 cm^{-1} shown in Figure 2. With further heating beyond 300 $^\circ\text{C}$, however, the difference in mass change becomes more remarkable when both samples underwent the second stage of mass loss. This suggests that once the unhydrolyzed alkoxy groups had been decomposed, there occurred a higher number of organic segments, dissociated from the inorganic networks in the former. This is further supported by the reduced amount of char yields at 850 $^\circ\text{C}$ produced by this sample, suggesting a lower number of remaining organic moieties that could be trapped in the inorganic network. Based on this observation, it is confirmed that a lower concentration of coupling agent can lessen the binding strength between the inorganic and organic moieties upon heating, particularly at temperatures beyond the decomposition temperature T_d of PMMA matrix (345 $^\circ\text{C}$).

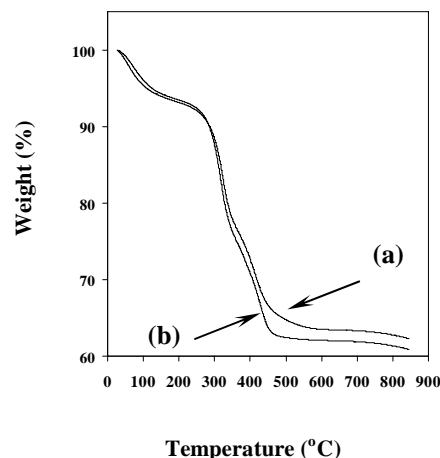


Figure 4. TGA curves of the nanohybrid derived from MSMA/(MSMA+MMA) ratio of (a) 0.25 and (b) 0.05, respectively.

Effect of pH value. Brinker and Hurd [14] and Langlet *et al.* [15] proposed that the amorphous state of TiO_2 was caused by the formation of stiff Ti–OH arising from fast condensation. In line with this understanding, Yoldas [17] also suggested that if the rate of condensation process is faster than hydrolysis, the alkyl groups are incorporated into the structure and sterically hinder the formation of

ordered structure. Therefore, in order to enable the precursor to crystallize into an equilibrium structure, the condensation should proceed slowly after the completion of hydrolysis. Lowering the pH value of the titania solution has been considered effective in enhancing the rate of hydrolysis and to inhibit the condensation [18]. This is made possible since the $-OR$ groups in alkoxide are protonated by H^+ ions, making their charges more positive. Being positively charged, the metal ions repel the $-OR$ groups and prefer to be attached to the $-OH$ groups. Consequently, this promotes the hydrolysis process and at the same time decreases the rate of condensation significantly since the protonated species reduce their interaction by repelling each other. Yoldas [19] and Kallala *et al.* [20] have shown a difference in the inhibition ratios can lead to sols, transparent gels, turbid gels or precipitates. Accordingly, Gopal *et al.* [21] and Watson *et al.* [22] have reported the formation of anatase and rutile TiO_2 synthesized directly from an acid-catalyzed solution at temperatures close to room temperature. For the nanohybrids investigated in this study, however, a question remains as to whether a slow condensation rate of the protonated titanium hydroxide can lead to the densification of TiO_2 during the subsequent annealing process, while at the same time polymerization of the MMA monomers takes place effectively. The latter is responsible for the fast trapping effect causing a largely amorphous TiO_2 phase in the polymer matrix. Therefore, it will be of further interest to investigate the effect of pH value on the nanocrystallinity of TiO_2 phase in nanohybrids. For the investigation, TiO_2 -PMMA nanohybrids were derived from TiO_2 sol solutions of pH value varying in the range of 3.08 to 0.33. This was done by adjusting the amount of hydrochloric acid (HCl) added, the function of which is to control the hydrolysis and condensation rates of titanium alkoxide [20,23]. The water to titanium alkoxide ratio (r_w) in each solution was kept at 0.82. Prior to mixing with the organic constituent, the sols were stirred at room temperature for 72 hours, aimed at providing sufficient time for the protonation of titanium alkoxide to take place, in accordance with the amount of hydrochloric acid added into the sol precursors. The XRD traces of the thus derived nanohybrids are given in Figure 5. It is shown that the nanohybrid derived from the inorganic sol solution of pH 3.08 (trace "(a)") is highly amorphous as indicated by the occurrence of two broadened humps in the 2θ ranges of 20–35° and 40–55°. By contrast, diffraction peaks

at 2θ of ~25 and 48° corresponding to (101) and (200) crystal planes of anatase titania were observed for the nanohybrids derived from the inorganic sol solution of pH 1.08 and 0.33 (traces "(b)" and "(c)").

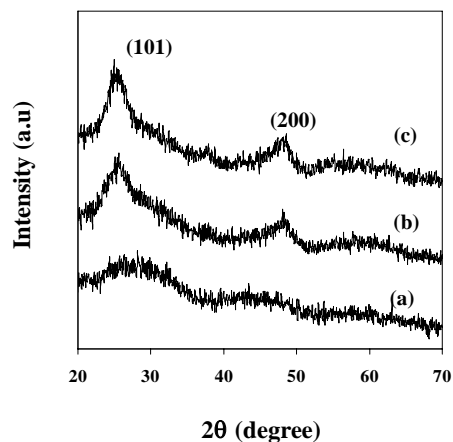


Figure 5. XRD traces of the nanohybrid derived from inorganic sol solution with pH value of (a) 3.08, (b) 1.08, and (c) 0.33, respectively.

The results observed above can be interpreted by considering the role of H^+ ion in providing repulsion forces among the protonated inorganic species. It is known that a highly acidic protonation leads to a stronger repulsion force and thus formation of extended structure from the hydrolyzed alkoxide [24]. By using small-angle X-ray scattering (SAXS), Xiong *et al.* [25,26] investigated the structure of inorganic species in trialkoxysilane-capped acrylic-titania hybrids derived from titania sols under three typical pH values of 4.4, 7.0 and 8.8, representing acid, neutral, and basic conditions, respectively. They observed that under the basic condition the inorganic domains can reach a radius of gyration (R_g) and fractal dimension (D) of 7.3 nm and 1.35. However, under the acid condition, the values were only 2.4 nm and 0.18, respectively. The smaller sizes in the latter were associated with the restriction of inorganic chain-like structure into open regions of the mesh produced by the crosslinked polymers [25,26]. This was more or less similar to the situation of the amorphous nanohybrid derived from titania sol with a pH value of 3.08 investigated in the present work (trace "(a)" in Figure 5). On the other hand, however, the notable diffraction peaks in the XRD traces "(b)" and "(c)" for the nanohybrids derived from titania sols with a much lower pH value

(1.08 and 0.33) suggest a rather different mechanism in comparison to what has been proposed by Xiong *et al.* [25, 26] for acid catalyst condition. In the system investigated in this project, the linear chain-like structures of hydrolyzed inorganic precursors were able to perform further self-densification in the solution stage. It proceeded up to the stage when the nanohybrid sample was annealed, whereby a rigid organic PMMA network was formed. The nanocrystallinity of the sample derived from the sol solution with a much lower pH value, *i.e.*, 0.33 (trace “(c)”) is slightly higher than that of 1.08 (trace “(b)”). It suggests that the stronger repulsion force created among the protonated species at lower pH values can induce a better densification for titania phase in the TiO₂-PMMA nanohybrid system.

Effect of water to alkoxide ratio. The water to alkoxide (R_w) or often called as *hydrolysis ratio* determines the potential functionality of inorganic monomers in building the network [27]. In the previous investigation, a R_w of 0.82 was consistently used for the titania sol which is stable and did not turn into a gel, prior to mixing with polymer matrix. However, this ratio is less than the required stoichiometric value, *i.e.*, 4. As a result, the alkoxide precursor experienced an incomplete hydrolysis process. It is therefore of interest to find out whether the amount of water during sol preparation can favor a more completed hydrolysis and thus provide a higher nanocrystallinity for the titania phase in nanohybrid. For investigation, three different sols with R_w of 0.82, 2.00 and 3.50 under the same pH value of 0.78 were prepared. All the titania sol solutions were transparent and stable. An attempt to increase R_w to 4.00 led to the formation of immediate gel which could not be incorporated homogeneously into pre-polymerized PMMA. Therefore, the first three compositions were used for further investigation. The XRD traces of the resulting nanohybrids are given in Figure 6. It is shown that when R_w is 0.82, the resulting nanohybrid (trace “(a)”) demonstrates two broadened diffraction peaks at 2θ of $\sim 25.35^\circ$ and 48.12° corresponding to (101) and (200) crystal planes of anatase titania phase. An increase in R_w to 2.00 did not lead to a significant enhancement in nanocrystallinity for the respective nanohybrid (trace “(b)”). However, there was an onset of additional two peaks at 2θ of 38.63° and 55.08° corresponding to (112) and (211) crystal planes.

Further increase of R_w to 3.50 gave rise to an unexpected occurrence of amorphous titania phase. The above observation can be analyzed by considering that an increase in R_w gives rise to a stronger nucleophilic reaction between water and alkoxide species, and thus more -OR groups bonded to metal were substituted by -OH network structure. A larger and more compact structure of inorganic domains, as a result of the formation of a three-dimensional network structure, is therefore expected with the completion of -OH network [25,26].

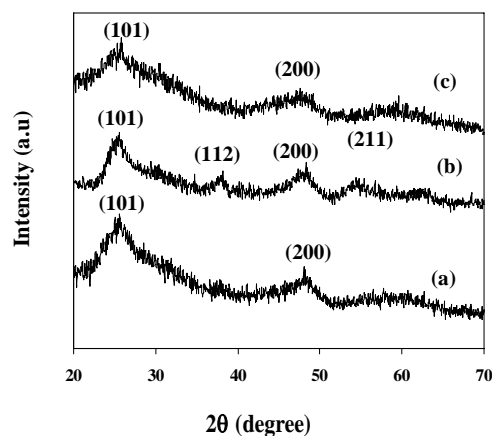


Figure 6. XRD traces of the nanohybrid derived from inorganic sol solution with R_w of (a) 0.82, (b) 2.00, and (c) 3.50, respectively.

Based on the XRD results, however, such increase in the inorganic domain size to form bigger nanocrystallites was not clearly indicated when R_w was increased from 0.82 to 2.00, as shown by diffraction peaks intensity at 2θ of $\sim 25.35^\circ$ and 48.12° . Yu *et al.* [28] has proposed a transition model of the inorganic domains in TiO₂-SiO₂ nanohybrid whereby chain-like structures transformed into particle-like clusters when R_w was varied from a value below the stoichiometric ratio (<4) to that of above the critical value (>4). The appearance of two additional peaks at 2θ of 38.63° and 55.08° suggested that the high number of -OH groups generated at R_w of 2.00 had provided more TiO₂ nuclei which furthermore grew as nanocrystals of different directions in addition to what has been formed at R_w of 0.82. It is of interest to compare the current result with a previous work performed by Xiong *et al.* [29] who employed SAXS technique to investigate the effect of water content on the structures of thermoplastic acrylic resin-titania hybrids. They

observed that hybrids derived from R_w of 1 and 2 demonstrated shallow linear regions in the Guinier and Porod plots, indicating little phase separation. Besides, the difference in scattering intensity between hybrids derived from R_w of 1 and 2 was small. This is very similar to the nanohybrids with R_w of 0.82 and 2 in the present study, as revealed by XRD results in Figure 6. However, at high R_w , a discrepancy occurs between the current result and what has been observed by Xiong *et al.* [29]. In their case, further increase of R_w up to 4 led to a denser inorganic phase with a larger size. In contrast, the nanohybrid derived from the hydrolysis ratio, R_w of 3.50, is highly amorphous when compared with those of derived from 0.82 and 2.00. Again, this is associated with the trapping of the hydrolyzed alkoxide groups by rigid PMMA network during and after annealing at 150 °C. It is highly possible that although a great number of -OH groups were generated through the relatively complete hydrolysis, however due to the strong constraint effect by organic polymer matrix, they failed to proceed to the subsequent densification and hence nanocrystalline TiO₂ phase was not achieved. In connection with the discrepancy observed between the two studies, it should be noted that Xiong *et al.* [25,26,29] relied on the SAXS scattering patterns in order to determine the sizes of inorganic phase in the hybrid composition. Indeed, several variations in their synthesis process such as pH value, water content and solvent mixture which led to different levels of hydrolysis and condensation for titania precursor could result in different levels of phase separation and thus scattering patterns accordingly. It was not confirmed whether the inorganic network formed in the hybrids were amorphous Ti-OH, nanocrystalline TiO₂ or a mixture of both. Therefore, the observed scattering pattern can be considered as a response from cumulative quantity of inorganic phases, regardless of their amorphous or crystalline nature. As a result, the SAXS studies of Xiong *et al.* [25,26,29] were not affected by the trapping mechanism of titania phase by the polymer matrix, as encountered in the nanohybrids investigated in the current study.

4. CONCLUSION

In an attempt to understand the mechanism responsible for the largely amorphous nature of the TiO₂ phase in the nanohybrids, several processing parameters involved in sol-gel and *in situ* polymerization were investigated, including

coupling agent concentration, pH value and water to alkoxide ratio. Variation of these processing parameters did not effectively lead to a significant enhancement in the nanocrystallinity of TiO₂ phase in the nanohybrids. They were not adequately effective to compete with the formation of stiff Ti-OH structures, which were trapped by the rigid network of polymerized PMMA matrix. This mechanism has resulted in a largely amorphous structure for TiO₂ phase in nanohybrids.

REFERENCES

1. H.A. Hornak, Ed. *Polymers for Lightwave and Integrated Optics*, Marcel Dekker, New York, 1992
2. J. Zhang, S. Luo and L. Gui, *J. Mater. Sci.* **32**, 1469 (1997)
3. W. C. Chen, S. J. Lee, L.H. Lee and J. L. Lin, *J. Mater. Chem.* **9**, 2999, (1999)
4. L. H. Lee and W.C. Chen, *Chem. Mater.* **13**, 1137 (2001)
5. A.H. Yuwono, J.M. Xue, J. Wang, H.I. Elim, W. Ji, Y Li and T.J. White, *J. Mater. Chem.* **13**, 1475 (2003).
6. H.I. Elim, W. Ji, A.H. Yuwono, J.M. Xue, J. Wang, *Appl. Phys. Lett.*, **82** (16), 2691 (2003).
7. B. Wang, G.L. Wilkes, J.C. Hedrick, S.C. Liptak and J.E. McGrath, *Macromolecules*, **24**, 3449 (1991).
8. G.L. Fischer, R.W. Boyd, R.J. Gehr, S.A. Jenekhe, J.A. Osaheni, J.E. Sipe and L.A. Weller-Brophy, *Phys. Rev. Lett.* **74** (10), 1871 (1995).
9. Y. Djaoued, S. Badilescu, P.V. Ashrit, D. Bersani, P.P. Lottici and R. Brüning, *J. of Sol-Gel. Sci. Tech.* **24**, 247 (2002).
10. S.X. Wang, M.T. Wang, Y.Lei and L.D. Zhang, *J. Mater. Sci. Lett.* **18**, 2009 (1999).
11. A. Leautic, F. Babonneau and J. Livage, *Chem. Mater.* **1**, 240 (1989).
12. W. Que, Y. Zhou, Y.L. Lam, Y.C. Chan, S.D. Cheng, Z. Sun and C.H. Kam, *J. Sol-Gel. Sci. Technol.* **18**, 77 (2000).
13. J. Zhang, X. Ju, B.J. Wang, Q.S. Li, T. Liu and T.D. Hu, *Synth. Met.* **118**, 181 (2001).
14. C.J. Brinker and A.J. Hurd, *J. Phys. III France* **4**, 1231 (1994).
15. M. Langlet, M. Burgos, C. Couthier, C. Jimenez, C. Morant and M. Manso, *J. Sol-Gel. Sci. Technol.* **22**, 139 (2001).
16. X.C. Chen, *J. Mater. Sci. Lett.* **21**, 1637 (2002).
17. B.E. Yoldas, *J. Mater. Sci.* **14**, 1843 (1979).
18. J. Livage, M. Henry and C. Sanchez, *Prog. Solid State Chem.* **18**, 259 (1988).
19. B.E. Yoldas, *J. Mater. Sci.* **21**, 1086 (1986).
20. M. Kallala, C. Sanchez and B. Cabane, *J. Non-Crys. Solids* **147-148**, 189 (1992).

21. M. Gopal, W.J. Moberly Chan and L.C. De Jonghe, *J. Mater. Sci.* **32**, 6001 (1997).
22. S. Watson, D. Beydoun, J. Scott and R. Amal, *J. Nanopart. Res.* **6**, 193 (2004).
23. M. Burgos and M. Langlet, *Thin Solid Films* **349**, 19 (1999).
24. C.L. Chiang, C.C. Ma, D. L. Wu and H.C. Kuan, *J. Polym. Sci. Polym. Chem.* **41**, 905 (2003).
25. M. Xiong, S. Zhou, L. Wu, B. Wang and L. Yang, *Polymer* **45**, 8127 (2004).
26. M. Xiong, S. Zhou, B. You and L. Wu, *Polymer* **43**, 637 (2005).
27. M. Kallala, C. Sanchez and B. Cabane, *Phys. Rev. E* **48**, 3692 (1993).
28. H. F. Yu and S.M. Wang, *J. Non-Cryst. Solids* **261**, 260 (2000).
29. M.N. Xiong, S.X. Zhou, B.You, G.X. Gu, L.M. Wu, *J. Polym. Sci. Polym. Phys.* **42**, 3682 (2004).